Rapid Communications

Validity of the Mott formula and the origin of thermopower in π-conjugated semicrystalline polymers

Shun Watanabe,[1,2,3,*] Masahiro Ohno,[1] Yu Yamashita,[1] Tsubasa Terashige,[1,2] Hiroshi Okamoto,[1,2] and Jun Takeya[1,2,4]

[1]*Material Innovation Research Center (MIRC) and Department of Advanced Materials Science, Graduate School of Frontier Sciences, The University of Tokyo, 5-1-5 Kashiwanoha, Kashiwa, Chiba 277-8561, Japan*

[2]*AIST-UTokyo Advanced Operando-Measurement Technology Open Innovation Laboratory (OPERANDO-OIL), National Institute of Advanced Industrial Science and Technology (AIST), 5-1-5 Kashiwanoha, Kashiwa, Chiba 277-8561, Japan*

[3]*JST, PRESTO, 4-1-8 Honcho, Kawaguchi, Saitama 332-0012, Japan*

[4]*International Center for Materials Nanoarchitectonics (WPI-MANA), National Institute for Materials Science (NIMS), 1-1 Namiki, Tsukuba 305-0044, Japan*

(Received 17 March 2019; published 18 December 2019)

Charge and thermoelectric transport should be closely correlated with each other; however, little is known regarding the origin of thermopower in semicrystalline π-conjugated polymers, particularly those doped with molecular dopants. It is controversial whether the well-established Mott formula is valid for such conducting polymers, which inevitably have a finite structural disorder. We show that a truly metallic regime that can be realized in a highly crystalline domain gives rise to thermopower, which is demonstrated unambiguously by the observation of a linear temperature dependence of the Seebeck coefficient in semicrystalline polythiophene-based conducting polymers. The presence of onset metallicity is also verified comprehensively by the Hall effect and Drude optical response, which indicates that the Mott formula, which is frequently used for degenerated semiconductors and metals, can be applicable to highly crystalline conjugated polymers. This provides insight into the structure-thermoelectric property relationships in semicrystalline conducting polymers.

DOI: 10.1103/PhysRevB.100.241201

The Seebeck coefficient is consistent thermodynamically with the amount of entropy accompanied by the flow of charge in a material. Entropy for electrons is confined to the electrochemical potential; therefore, an in-depth understanding of electronic band structure would provide a fundamental guide to thermoelectric properties. In a typical metal and degenerated semiconductor, the electrochemical potential lies within a delocalized band, where only a fixed population of electrons with the Fermi energy close to a few k_BT contributes to both charge and thermoelectric transport. Narrowing of the Fermi-Dirac distribution towards lower T results in a linear decrease of the Seebeck coefficient with T. Under the rigid band approximation, the Mott formula is often employed for interpretation of the thermopower S [1,2],

$$S = -\frac{\pi^2 k_B^2 T}{3e}\left[\frac{d\ln\sigma_E}{dE}\right]_{E=E_F}, \tag{1}$$

where $\sigma_E(E)$ denotes a transport function at a given energy level E. In an intrinsic or lightly doped semiconductor, mobile electrons should obey the Boltzmann statistics, so that the electrochemical potential lies within a band gap; therefore, the energy difference between the electrochemical potential and the occupied level defines the Seebeck coefficient [3,4]. Given the Kelvin relation, the Seebeck coefficient is proportional to the inverse temperature, i.e., $S \propto T^{-1}$ [5,6].

The Mott formula shown in Eq. (1) gives a convenient guide to not only understand the thermoelectric properties, but also to search for candidate thermoelectric materials [7]. The Mott formula can be applicable to metals and degenerate semiconductors, where electron transport occurs only near the Fermi level, i.e., the occupation of electrons follows the Fermi-Dirac statistics. In addition to this, the transport function σ_E should change weakly around the chemical potential in the range of a few k_BT. Under the rigid band approximation in conjunction with the Boltzmann transport framework, $\sigma_E(E)$ is given by the product of the energy-dependent relaxation time $\tau(E)$, the velocity of the mobile carrier $v(E)$, and the density of states (DOS) $N(E)$ [i.e., $\sigma_E(E) = \frac{e^2}{3}\tau(E)v^2(E)N(E)$] [1,2]. From this assumption, in Eq. (1), a steep change in $\frac{d\ln\sigma_E}{dE} \approx \frac{d\ln N}{dE}$ near E_F gives an increase in S. This fact has motivated a usage of low-dimensional materials, where their density of states is likely to possess a nonuniform profile in energy space [7,8]. In a similar fashion, the Mott formula has been frequently employed with organic thermoelectric materials to interpret their thermoelectric properties and to design high-performance organic compounds [9–11]. However, it is controversial whether the Mott formula is valid in organic materials, particularly in conjugated polymers, and it is more reasonable to envisage that the Mott formula is violated due to the following reasons. First, charge transport in such conducting polymers is likely to undergo hopping transport between localized states, which results in the failure of the rigid band approximation. Second, localized tail states are likely to result in E_F being pinned deep in the band

*Correspondence and requests for materials should be addressed to swatanabe@edu.k.u-tokyo.ac.jp

gap, even though the carrier filling is controlled by doping. Both phenomena originate from the noncrystalline nature of conducting polymers, i.e., structural disorder inevitably found in conducting polymers.

Thermoelectric applications using polymeric semiconductors are being studied actively and are recognized as a cutting-edge application of the next generation of printing electronics [12–15]. However, there is no clear guideline for material design to aim for highly efficient thermoelectric properties in organic semiconductors with a concomitant finite disorder, both in the crystal structure and in the energy space. In particular, the correlation between the characteristic microcrystallinity of polymeric semiconductors and thermoelectric properties has not yet been clarified; how the nonuniformity of the DOS in the energy space has an impact on thermoelectric power, and to what extent the thermoelectric properties of organic semiconductors can be improved by materials science remain unclear. Thermopower is governed predominantly by a reduced chemical potential. Many of the previous studies have already shown changes in thermopower for such disordered materials with respect to changes in the Fermi energy by carrier filling, i.e., by chemical doping [16–18]. In addition to carrier filling, the assessment thermopower with a temperature variation provides an in-depth understanding of the thermoelectric properties due to modulation of the reduced chemical potential, which is generally more effective rather than carrier filling. However, little is known to date regarding the temperature dependence of the Seebeck coefficient in thin films of conducting polymers.

In this Rapid Communication, we present the temperature dependence of electrical conductivity and the Seebeck coefficient in a semicrystalline conjugated polymer, PBTTT [poly(2, 5-bis(3-alkylthiophen-2-yl)thieno [3, 2-*b*]thiophene)], that is chemically doped with various molecular dopants. Details of the materials and doping methods are given in the Supplemental Material [19]. The charge transport mechanism varies depending on the doping level, i.e., from thermal activation at lower doping levels to variable-range hopping at higher doping levels. In striking contrast, the Seebeck coefficient shows a linear temperature dependence, predicted by the Mott formula in Eq. (1), independent of the doping level. This clearly indicates that a truly metallic regime that can be realized in highly crystalline domains in PBTTT gives rise to thermopower, and that the Mott formula is valid in such conducting polymers.

To assess the thermoelectric properties in conducting polymers, the well-established methodology employed in previous studies [22,23] was followed. Figure 1 shows an optical microscope image of the microfabricated, on-chip thermometry device used in the present work, where Cr (3 nm) and Au (30 nm) electrodes are patterned as a heater, temperature sensor, and potential probes. This on-chip thermoelectric measurement is applicable for a wide temperature range down to approximately 30 K. Pairs of longitudinal and transverse potential probes are patterned across the channel to accurately measure four-point-probe conductivity σ and the Hall coefficient R_{H}. The demonstrated configuration allows simultaneous measurement of the conductivity, Seebeck coefficient, and Hall carrier density. Details of the fabrication process are given in the Supplemental Material [19].

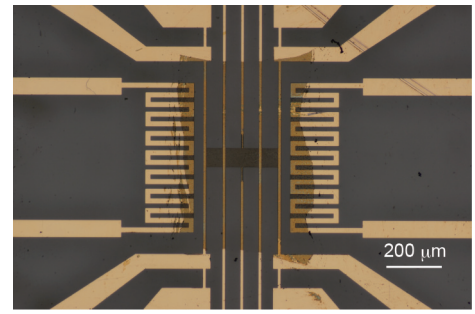

FIG. 1. Optical microscope image of a thermoelectric device of PBTTT thin film with a thickness of 40 nm. The channel length and width are designed to be 300 and 80 μm, respectively. Note that a layer of doped PBTTT is patterned via laser etching, such that no overlaps with the heater are established to ensure electrical isolation between the heater and the sensors.

A layer of doped PBTTT was spin coated onto the chip from a solution of 1, 2-dichlorobenzene and was patterned into an active island. Here, we intentionally fabricated three different samples with different conductivities via chemical doping. The sample with the lowest conductivity at room temperature ($\sigma^{\mathrm{RT}} \sim 10^{-1}$ S cm^{-1}; solution doped) was fabricated via codeposition of an acceptor dopant [tetrafluorotetracyanoquinodimethane (F_4-TCNQ)] with the polymer from solution [26]. The sample with $\sigma^{\mathrm{RT}} \sim 100$ S cm^{-1} (vapor doped) was fabricated via vapor deposition of F_4-TCNQ on top of the PBTTT thin film. This allows the F_4-TCNQ molecules to intercalate into the film, which results in PBTTT retaining its highly ordered, lamellar microstructure [27,28]. The sample with the highest conductivity ($\sigma^{\mathrm{RT}} \sim$ 350 S cm^{-1} at 300 K; anion exchanged [29]) was fabricated via anion-exchange doping. In contrast to conventional molecular doping, we recently demonstrated anion-exchange doping to improve the level of molecular doping, where radical anions based on small molecules, acceptor dopants (e.g., F_4-TCNQ), are incorporated into the polymer film and exchanged instantaneously for an additive anion [e.g., a closed shell ion, bis(trifluoromethylsulfonyl)imide, $TFSI^-$]. By controlling the ionic interaction, the anion exchange reaches 100% efficiency, so that the molecular doping approached a doping level of one hole per monomer unit. Note that with given doping methods, dopants intercalate into the entire bulk of the PBTTT layer, which was verified by x-ray reflectivity measurements (see more details in the Supplemental Material [19]).

Figure 2(a) shows the temperature T dependence of four-point-probe conductivity for three samples with different σ^{RT}. Variation of the dopant and doping methodology has an effect on not only the room-temperature conductivity, but also on the charge transport mechanism. For the solution-doped sample (black symbols), charge transport is governed predominantly by hopping, i.e., the thermally activated tunneling of carriers between localized states. For the vapor-doped and anion-exchanged samples, the decrease in σ with a decrease in T is much weaker. To analyze the data, we use the concept of variable-range hopping (VRH), i.e., a carrier may either hop over a small distance with a high activation energy or hop over a long distance with a low activation energy [6,32–34].

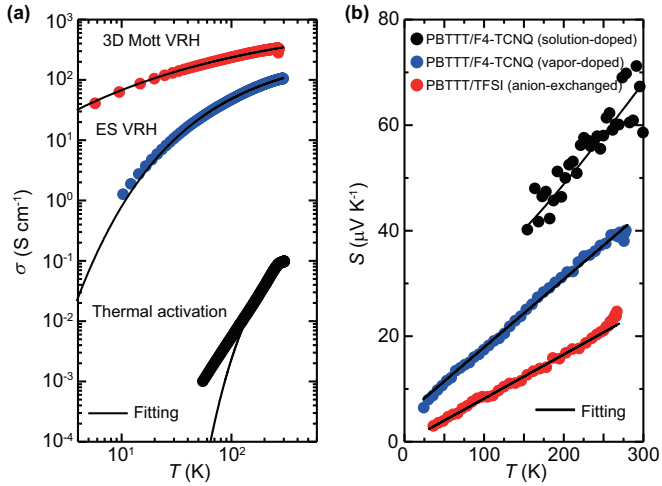

FIG. 2. Temperature dependence of (a) four-point-probe conductivity and (b) Seebeck coefficient for doped PBTTT thin films with three different doping levels. Solid lines represent fitting results. The discrepancy between the experimental data and fitting result specifically found at low temperatures in the solution-doped sample may be due to the contribution of field-assisted tunneling becoming dominant at low temperatures, which is consistent with recent theoretical and experimental studies [30,31]. The maximum compound error in S that results from propagation of the uncertainties in the thermal voltage and ΔT was evaluated to be 3 μV K^{-1} (see more details in the Supplemental Material [19]).

The temperature dependence of the carrier transport analyzed based on VRH model is expressed as

$$\sigma(T) = \begin{cases} \sigma_0 \exp\left[-\left(\frac{T_0}{T}\right)^{\frac{1}{d+1}}\right] & \text{(Mott-VRH)}, \quad (2a) \\ \sigma_0 \exp\left[-\left(\frac{T_0}{T}\right)^{\frac{1}{2}}\right] & \text{(ES-VRH)}, \quad (2b) \\ \sigma_0 \exp\left(-\frac{T_0}{T}\right) & \text{(Arrhenius)}, \quad (2c) \end{cases}$$

where σ_0 is the high-temperature limit of conductivity and T_0 is a characteristic temperature. In the general Mott-VRH model, d represents the dimensionality of charge transport, i.e., $d = 3$ for three-dimensional VRH [Eq. 2(a)]. When taking into account Coulombic interactions between localized sites, a soft gap appears in the DOS near the Fermi energy. The modification from pure Mott VRH yields the Efros-Shklovskii VRH (ES-VRH) model, which predicts $d = 1$ [Eq. 2(b)], regardless of dimensionality [34]. We find that the localized transport models summarized in Eq. (2) give a better fit for the temperature dependence of conductivity [Fig. 2(a)]. For the solution-doped sample with the lowest σ^{RT} of 10^{-1} S cm^{-1} at room temperature, the temperature dependence of σ follows a thermal activation process [Eq. 2(c)], which is consistent with the previous studies [27,32,33]. As the doping level increases, VRH becomes dominant. The experimental data can be fitted almost perfectly with $d = 1$ for the vapor-doped sample with $\sigma^{\mathrm{RT}} = 100$ S cm^{-1}, and with $d = 3$ for the anion-exchanged sample with $\sigma^{\mathrm{RT}} = 350$ S cm^{-1} (see more details in the Supplemental Material [19]). We do not speculate here on the transition of the charge transport mechanism with respect to the doping level, but merely note that the transition from ES-VRH to Mott-VRH has been observed with an increased doping level [27,32,33].

In striking contrast to the temperature dependence of σ, where a clear transition from thermal activation to VRH was observed as the doping level increases, a universal temperature dependence on the Seebeck coefficient, i.e., a linear temperature dependence ($S \propto T$), was experimentally obtained for the three different samples [Fig. 2(b)]. Note that depending on the charge transport models, the temperature variation in S is known to be different, as expected [2,3],

$$S(T) \propto \begin{cases} T^{\frac{d-1}{d+1}} & \text{(Mott-VRH)}, \quad (3a) \\ S_0 & \text{(ES-VRH)}, \quad (3b) \\ T^{-1} & \text{(Arrhenius)}. \quad (3c) \end{cases}$$

The experimentally observed temperature dependence of σ is always unlike that expected in a metal, which causes a conceptional failure of the validity of the Mott formula. However, the temperature dependence of S is unexpectedly linear and independent of the charge transport models.

The observed linear temperature dependence is interpreted using the Mott formula shown in Eq. (1). This indicates that an electromotive force due to the Seebeck effect arises from a truly metallic domain in PBTTT, i.e., both the rigid band approximation and Boltzmann transport hold in the highly crystalline domains of PBTTT. The difference in slope for different samples corresponds to $[\frac{d \ln \sigma_{\mathrm{E}}}{dE}]_{E=E_{\mathrm{F}}}$ in Eq. (1), and can be explained by carrier filling. At low doping levels, a large slope is obtained due to the steep increase of the DOS in the energy space (likely because E_{F} positions at a steep tail state of the DOS). The energy dependence of the DOS becomes weaker as carrier filling proceeds, so the slope becomes small. The shape of the DOS in the energy space for doped PBTTT has yet to be clarified: Therefore, it cannot be said quantitatively, but the trend is consistent with that often observed in degenerate semiconductors [7,8]. The presence of onset metallicity is also verified comprehensively by the Hall effect and Drude optical response, as discussed later. Note that the linear T dependence of S at temperature regimes limited to above 100 K has been observed in a pellet shape of highly doped polyacetylene [35] and polyaniline [36]. However, the presence of such onset metallicity has been argued for many years, and little evidence of metallic conduction in such disordered polymers has been demonstrated. In this context, the observation of metallicity in PBTTT is reasonably understood by the highly crystalline domain of PBTTT, so that the rigid band theory in conjunction with the Boltzmann transport model, which relies fundamentally on a periodic crystal potential, can be applicable.

It is expected that the metallic thermopower is dominant even in systems that have both metallic and localized conduction. Previous studies have revealed that crystalline polymers have a characteristic microstructure in which the crystalline domains are intermittently connected [37,38], which means that their crystalline structure can be approximated to a polycrystal that includes a grain boundary. Because highly crystalline domains are not continuously formed between electrodes, charge transport and thermoelectric transport always occurs through the grain boundaries. The electrical conductivity of the grain boundary is significantly smaller than that of the crystalline domain, and shows a steep temperature dependence (the conductivity decreases exponentially

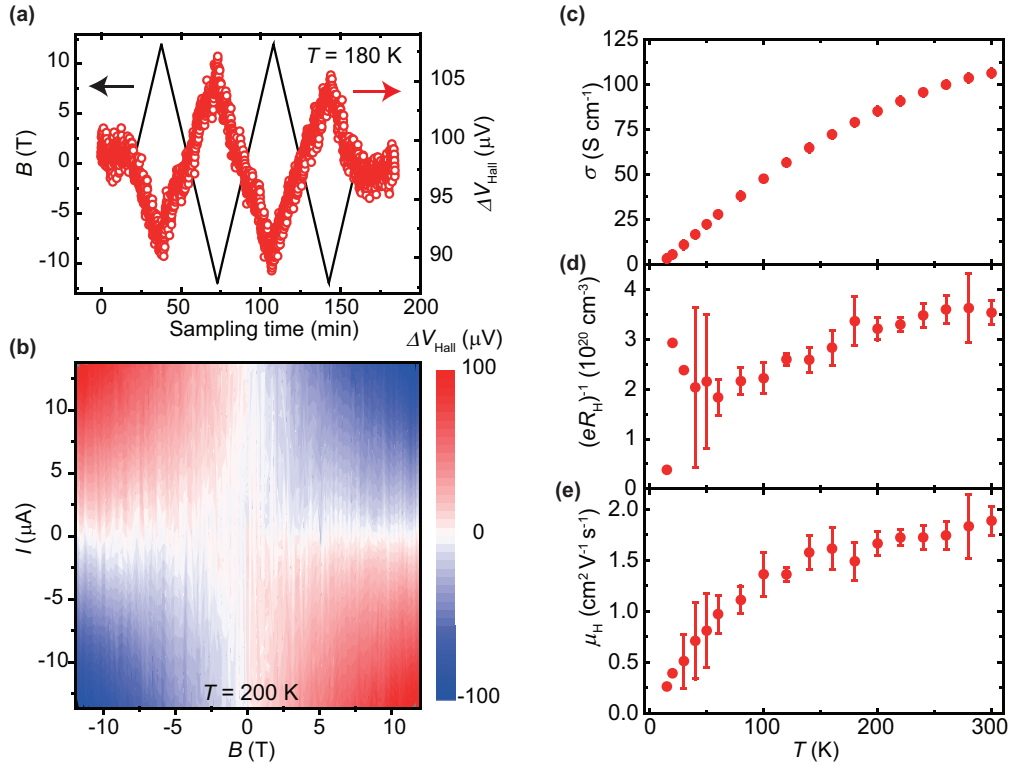

FIG. 3. (a) Evolution of the Hall voltage ΔV_{Hall}, measured with the thermoelectric device consisting of doped PBTTT thin film (F_4-TCNQ implanted) at 200 K. Measurements were taken with magnetic field B ramped up to 12 T and down to -12 T. (b) Contour plot of ΔV_{Hall} for different excitation currents I and B. Temperature T, dependence of (c) the conductivity σ, (d) the inverse Hall coefficient $(e|R_{\mathrm{H}}|)^{-1}$, and (e) the Hall mobility μ_{H}, estimated from $\mu_{\mathrm{H}} = |R_{\mathrm{H}}|\sigma$. The error bars represent uncertainty in the extraction of ΔV_{Hall} from the fitting.

with respect to the temperature); therefore, the total electrical conductivity is likely to be limited by the localized electrons in the grain boundary. This model has been referred to as multiple trap and release (MTR). The total thermopower is also expected to be a linear summation of the metallic and localized contributions. However, the temperature gradient that is effectively formed across the grain boundary, which can be considered as a line defect, is overwhelmingly small; therefore, we expect that metallic thermopower is dominant in the MTR system. Such a hybrid transport model that takes into account the grain boundary seems to explain the results at first glance; however, the total thermopower should be balanced delicately by the formation of crystalline domains and grain boundaries.

The delocalized charge transport can be directly confirmed and elaborated further by discussion of the Hall effect measured in the same sample on the on-chip thermometer device (Fig. 1) for the vapor-doped sample, and a typical Hall voltage with respect to ramping the magnetic field B, is shown in Fig. 3(a). A clear Hall voltage signal is observed over a wide range of temperatures from 300 to 20 K, which provides evidence for the metallic behavior of delocalized charge carriers. From the sign of the voltage, hole charge carriers are also confirmed [Fig. 3(b)]. The observed positive temperature coefficient of conductivity [Figs. 2(a) and 3(c)] does not contradict the existence of metallic states, because the Hall voltage can be generated by summing over the contributions from metallic grains where Hall voltages are produced, even if there are grain boundaries in between that prevent observation of a fully metallic longitudinal conductivity. The inverse Hall coefficient $(e|R_{\mathrm{H}}|)^{-1}$ and Hall mobility μ_{H}, derived in a standard manner, show a weak temperature dependence, which is consistent with previous studies [27]. The observed $(e|R_{\mathrm{H}}|)^{-1} \sim 3 \times 10^{20}$ cm^{-3} corresponds to 0.3 charge carriers per monomer unit of PBTTT. With this high carrier concentration, the localized trap DOS is likely to be filled because the transport level is close to the delocalized band edge. Although there remains a finite contribution of localized carriers that may become more dominant at lower temperatures, the main contributor for charge conduction is band carriers. This is also verified by observation of the Drude optical response in optical reflectivity measurements. Details of optical reflectivity measurements are given in the Supplemental Material [19] .

Lastly, we discuss how the linear T-temperature dependence of S can be related to a recent theoretical study with a plot of S vs σ [41]. Kang and Snyder have developed a universal charge and thermoelectric transport model to interpret a unique σ-S relation. In this model, $S \propto \sigma^{-\frac{1}{4}}$, which has been observed experimentally in many polymeric thermoelectric materials [14,42], was well explained by a transport function, $\sigma_{\mathrm{E}} = \sigma_{\mathrm{E}_0}(\frac{E-E_{\mathrm{t}}}{k_{\mathrm{B}}T})^s$, with a transport exponent of $s = 3$. We emphasized that the linear T dependence of S does not contradict this model and even validates it for the following reasons. First, the Kang-Snyder model holds only in the degenerate limit, and the Mott formula does likewise. The Fermi degeneracy in semicrystalline polymers is comprehensively verified experimentally by the observation of an almost ideal

Hall effect (Fig. 3), a Drude optical response, and Pauli paramagnetism [27]. Second, the Kang-Snyder model assumes a simplistic power law relation, $(\frac{E-E_t}{k_B T})^s$, in the transport function σ_E, as does the Mott formula. The linear T dependence of S that appears concomitantly with the inverse power relation $S \propto \sigma^{-\frac{1}{4}}$ is considered to originate from a unique structure in doped semicrystalline polymers with a finite amount of structural disorder, so that S and σ can be optimized separately by tuning these microcrystalline structures and their percolation behavior. We note that our finding can be applicable not only to PBTTT, but also to conducting crystalline polymers, as long as the conduction can be explained in the degenerate limit. The vast array of recent chemical doping methodologies will allow for the effective doping of crystalline polymeric semiconductors, and it will even be possible to achieve highly doped states that approach their degenerate limit. The present results provide important insight into the physical guidelines for further development and material design in the future.

In summary, the Seebeck coefficient in highly doped, semicrystalline PBTTT was measured down to low temperatures and a linear temperature dependence of the Seebeck coefficient observed, independent of charge transport models. The observation of an almost ideal Hall effect verified that metallic conduction domains do exist in the semicrystalline domains of PBTTT. The Mott formula, which is used frequently for degenerate semiconductors and metals, is confirmed to be also applicable to highly crystalline conjugated polymers. The Mott formula gives a convenient guide for the search of candidate thermoelectric materials, although it is likely applicable only to semicrystalline conducting polymers. The energy derivative of the logarithmic of the DOS, $\frac{d \ln N}{dE}$, in the expression clearly indicates that the Seebeck coefficient is not only a sensitive probe of electronic structure, but can also be improved by steeping the DOS near E_F. Polymeric materials that inherently have a one-dimensional nature can be advantageous in terms of their nonuniform DOS. In particular, control of the subthreshold regime of the DOS in the energy space may lead to large, controllable thermopower, which can be realized by microscopic ordering of the polymeric chains.

This work was supported by a Grant-in-Aid (No. JPMJPR151E) from the PRESTO program of the Japan Science and Technology Agency (JST) through the Hypernanospace Design Toward Innovative Functionality project, and by the Leading Initiative for Excellent Young Researchers of the Japan Society for the Promotion of Science (JSPS). This work was also supported in part by Kakenhi Grants-in-Aid (No. JP17H06123 and No. JP17H06200) from JSPS.

[1] M. Cutler and N. F. Mott, Phys. Rev. **181**, 1336 (1969).
[2] N. Mott and E. Davis, *Electronic Process in Non-Crystalline Materials* (Oxford University Press, Oxford, U.K., 1971).
[3] D. K. C. MacDonald, *Thermoelectricity: An Introduction to the Principles* (Wiley, New York, 1962).
[4] J. M. Ziman, *Principles of the Theory of Solids* (Cambridge University Press, Cambridge, U.K., 1964).
[5] H. Fritzsche, Solid State Commun. **9**, 1813 (1971).
[6] I. Zvyagin, Phys. Status Solidi B **58**, 443 (1973).
[7] D. M. Rowe, *Materials, Preparation, and Characterization in Thermoelectrics* (CRC Press, Boca Raton, FL, 2017).
[8] L. D. Hicks and M. S. Dresselhaus, Phys. Rev. B **47**, 16631 (1993).
[9] Y. W. Park, W. K. Han, C. H. Choi, and H. Shirakawa, Phys. Rev. B **30**, 5847 (1984).
[10] C. Yoon, M. Reghu, D. Moses, A. Heeger, Y. Cao, T.-A. Chen, X. Wu, and R. Rieke, Synth. Met. **75**, 229 (1995).
[11] M. He, F. Qiu, and Z. Lin, Energy Environ. Sci. **6**, 1352 (2013).
[12] O. Bubnova and X. Crispin, Energy Environ. Sci. **5**, 9345 (2012).
[13] B. Russ, A. Glaudell, J. J. Urban, M. L. Chabinyc, and R. A. Segalman, Nat. Rev. Mater. **1**, 16050 (2016).
[14] E. M. Thomas, B. C. Popere, H. Fang, M. L. Chabinyc, and R. A. Segalman, Chem. Mater. **30**, 2965 (2018).
[15] N. Lu, L. Li, and M. Liu, Phys. Chem. Chem. Phys. **18**, 19503 (2016).
[16] O. Bubnova, Z. U. Khan, A. Malti, S. Braun, M. Fahlman, M. Berggren, and X. Crispin, Nat. Mater. **10**, 429 (2011).
[17] G. H. Kim, L. Shao, K. Zhang, and K. P. Pipe, Nat. Mater. **12**, 719 (2013).
[18] O. Bubnova, Z. U. Khan, H. Wang, S. Braun, D. R. Evans, M. Fabretto, P. Hojati-Talemi, D. Dagnelund, J.-B. Arlin, Y. H. Geerts *et al.*, Nat. Mater. **13**, 190 (2014).
[19] See Supplemental Material at http://link.aps.org/supplemental/10.1103/PhysRevB.100.241201 for details of materials and doping methods, the fabrication process, and the optical reflectivity measurements, which includes Refs. [16,20–25,39,40].
[20] I. McCulloch, M. Heeney, C. Bailey, K. Genevicius, I. MacDonald, M. Shkunov, D. Sparrowe, S. Tierney, R. Wagner, W. Zhang *et al.*, Nat. Mater. **5**, 328 (2006).
[21] I. E. Jacobs, E. W. Aasen, J. L. Oliveira, T. N. Fonseca, J. D. Roehling, J. Li, G. Zhang, M. P. Augustine, M. Mascal, and A. J. Moulé, J. Mater. Chem. C **4**, 3454 (2016).
[22] D. Venkateshvaran, M. Nikolka, A. Sadhanala, V. Lemaur, M. Zelazny, M. Kepa, M. Hurhangee, A. J. Kronemeijer, V. Pecunia, I. Nasrallah *et al.*, Nature (London) **515**, 384 (2014).
[23] M. Yoshida, T. Iizuka, Y. Saito, M. Onga, R. Suzuki, Y. Zhang, Y. Iwasa, and S. Shimizu, Nano Lett. **16**, 2061 (2016).
[24] J. Liu, X. Wang, D. Li, N. E. Coates, R. A. Segalman, and D. G. Cahill, Macromolecules **48**, 585 (2015).
[25] Q. Wei, M. Mukaida, K. Kirihara, Y. Naitoh, and T. Ishida, Materials **8**, 732 (2015).
[26] J. E. Cochran, M. J. Junk, A. M. Glaudell, P. L. Miller, J. S. Cowart, M. F. Toney, C. J. Hawker, B. F. Chmelka, and M. L. Chabinyc, Macromolecules **47**, 6836 (2014).
[27] K. Kang, S. Watanabe, K. Broch, A. Sepe, A. Brown, I. Nasrallah, M. Nikolka, Z. Fei, M. Heeney, D. Matsumoto *et al.*, Nat. Mater. **15**, 896 (2016).
[28] R. Fujimoto, Y. Yamashita, S. Kumagai, J. Tsurumi, A. Hinderhofer, K. Broch, F. Schreiber, S. Watanabe, and J. Takeya, J. Mater. Chem. C **5**, 12023 (2017).
[29] Y. Yamashita, J. Tsurumi, M. Ohno, R. Fujimoto, S. Kumagai, T. Kurosawa, T. Okamoto, J. Takeya, and S. Watanabe, Nature (London) **572**, 634 (2019).

[30] L. Li, N. Lu, and M. Liu, J. Appl. Phys. **116**, 164504 (2014).
[31] A. M. Glaudell, J. E. Cochran, S. N. Patel, and M. L. Chabinyc, Adv. Energy Mater. **5**, 1401072 (2015).
[32] T. Harada, H. Ito, Y. Ando, S. Watanabe, H. Tanaka, and S.-i. Kuroda, Appl. Phys. Express **8**, 021601 (2015).
[33] S. Wang, M. Ha, M. Manno, C. D. Frisbie, and C. Leighton, Nat. Commun. **3**, 1210 (2012).
[34] A. Efros, N. Van Lien, and B. Shklovskii, Solid State Commun. **32**, 851 (1979).
[35] M. Przybylski, B. Bulka, I. Kulszewicz, and A. Proń, Solid State Commun. **48**, 893 (1983).
[36] E. Holland and A. Monkman, Synth. Met. **74**, 75 (1995).
[37] T. Schuettfort, B. Watts, L. Thomsen, M. Lee, H. Sirringhaus, and C. R. McNeill, ACS Nano **6**, 1849 (2012).
[38] O. Panova, C. Ophus, C. J. Takacs, K. C. Bustillo, L. Balhorn, A. Salleo, N. Balsara, and A. M. Minor, Nat. Mater. **18**, 860 (2019).
[39] H. Yamakawa, T. Miyamoto, T. Morimoto, T. Terashige, H. Yada, N. Kida, M. Suda, H. Yamamoto, R. Kato, K. Miyagawa *et al.*, Nat. Mater. **16**, 1100 (2017).
[40] K. Lee, S. Cho, S. H. Park, A. Heeger, C.-W. Lee, and S.-H. Lee, Nature (London) **441**, 65 (2006).
[41] S. D. Kang and G. J. Snyder, Nat. Mater. **16**, 252 (2017).
[42] S. N. Patel, A. M. Glaudell, K. A. Peterson, E. M. Thomas, K. A. O'Hara, E. Lim, and M. L. Chabinyc, Sci. Adv. **3**, e1700434 (2017).